Int. J. Solids Structures Vol. 15, pp. 111–126

0020-7683/79/0201-0111/$02.00/0

UNSTABLE GROWTH OF THERMALLY INDUCED INTERACTING CRACKS IN BRITTLE SOLIDS: FURTHER RESULTS

L. M. KEER, S. NEMAT-NASSER and A. ORANRATNACHAI
Department of Civil Engineering, Northwestern University, Evanston, IL 60201, U.S.A.

(*Received* 16 *February* 1978; *in revised form* 30 *May* 1978)

Abstract—This paper is complementary to a previous work[1] in which the growth and stability of a system of thermally induced equally spaced parallel edge cracks in a half-plane consisting of a homogeneous isotropic linearly elastic brittle solid has been studied. Initially the half-plane has a uniform temperature, and the edge cracks are introduced by continuous cooling of its free surface. The cracks grow into the solid at an equal rate with the increasing thickness of the thermal boundary layer which forms close to its free surface. However, because of the interaction between adjacent cracks, a critical state may be reached after which some of the cracks stop growing while the remaining ones grow at a faster rate. This new growth regime may again be interrupted at a new critical state where either the cracks which had stopped growing would then suddenly snap closed while the remaining cracks jump to a finitely longer length, or a different growth regime takes place, depending on the nature of the temperature profile. The present work is concerned with a careful examination of the growth regime at and after the above-mentioned *second* critical state. This examination requires consideration of three interacting unequal cracks which involves crack extension in both Modes I and II. As in[1] two different temperature profiles, relevant to the problem of heat extraction from hot dry rock masses, are considered. It is shown that when the temperature profile in the solid is in the form of an error function, the inclusion of the third interacting crack changes the previously obtained results qualitatively (i.e. no crack closure is attained in this case), whereas for the second temperature profile our new (more complicated) calculations only confirm the previously obtained results.

INTRODUCTION

Because of cooling, externally applied loads, residual-stress build-up due to creep, loss of moisture and consequent shrinkage, or other natural or imposed processes, cracks often form in solids. Problems of this kind include the formation of surface cracks in aging wood, thermal cracks in nuclear reactor fuel elements, shrinkage cracks in drying concrete, desiccation cracks in deserts and at the bottom of dried up lakes, to name just a few. Cracks of this type can be considered as being *strain* controlled rather than *stress* controlled. In strain controlled problems of this kind, there usually exists a natural mechanism for the cracks to be self-arresting, while no such mechanism is generally available in the stress controlled problems because, in a strain controlled problem the total elastic energy available to induce cracking is limited, whereas in the stress controlled case, the external load may provide the needed energy continuously.

Cracks governed by a strain controlled mechanism are often highly interacting, so that their growth pattern may involve unstable sequences of events. A problem of this type has recently been studied by Nemat-Nasser *et al.*[1], where a system of equally spaced parallel edge cracks induced in a half plane by cooling of the free surface, has been carefully studied.† The half plane in [1] is assumed to be a homogeneous, isotropic, linearly elastic, brittle solid. The cracks grow under the action of a prescribed temperature profile, and the depth, δ, in which most of the temperature gradient takes place is used as the "loading parameter".

It has been found in [1] for a collinear growth pattern that if the effect of crack interaction is not taken into account, then all cracks tend to grow equally as the loading parameter δ increases. This is the case described in Fig. 1(a), which shows a typical unit cell of the infinite array for a noninteracting crack system. The case of interacting cracks is shown in Fig. 1(b), in which the unit cell now consists of two cracks that may have different lengths. It should be noted that in both cases, when crack branching is excluded, and when the symmetry of the

†The basic stability theory for a system of interacting cracks (strain-controlled) was first given by Nemat-Nasser[2], and a brief account of the theory was reported by Keer *et al.*[3], and published by Nemat-Nasser[4]. The corresponding stability theory for interacting cracks in combined fracture modes is given by Nemat-Nasser[5].

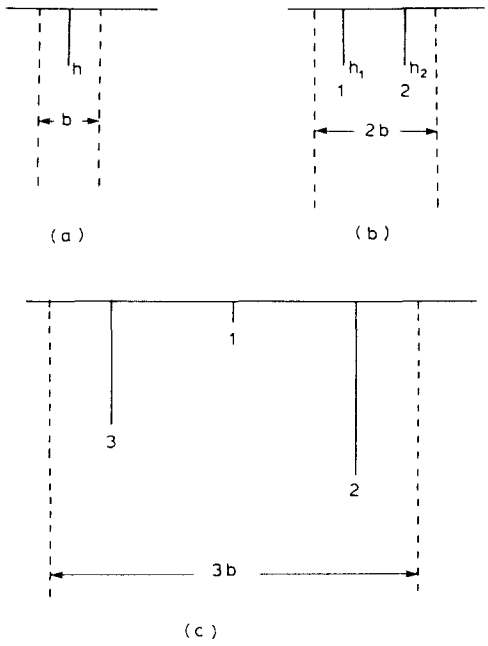

Fig. 1. (a) Unit cell for noninteracting cracks; (b) unit cell for two interacting cracks; (c) unit cell for three interacting cracks.

infinite crack array is exploited, only Mode I crack growth is possible. The case of two interacting cracks has been explored in detail in [1]. However, the possibility of three interacting cracks, whose unit cell is described by Fig. 1(c), has not been considered in [1] as it presented a computational complexity that seemed unnecessary to explore at the time. It should be noted that for the array whose unit cell is described by Fig. 1(c), the lack of symmetry about crack 1 implies that both Modes I and II exist at this crack, whereas cracks 2 and 3 have Mode I only; for the theory of stability of the growth of interacting cracks which involve all three modes (without branching) (see Nemat-Nasser[5]).

The present paper considers three interacting cracks and some of the results will show qualitative changes with one of the two problems considered in [1], although the essential features of the growth behavior remain the same. We note that the case of noninteracting cracks (Fig. 1a) can be considered a case of *constrained* stability which is corrected by the introduction of interacting cracks (Fig. 1b). In fact, it was shown in [1] that a system of noninteracting cracks is always stable for the considered temperature profiles. An analogy can be made between this problem and that of a shallow arch with a load acting at its center. If the arch is assumed to buckle symmetrically, then a critical value for the load can be obtained by a standard calculation. However, a lower value for the critical load is obtained if the antisymmetric buckling mode is also included. The constrained stability case for the arch is thus the one in which antisymmetrical displacements are excluded. Similarly, it will be shown here that the two crack system (Fig. 1b) represents a constrained stability state and that an instability due to three interacting cracks may manifest itself with a smaller critical load parameter, depending upon the temperature profile.

For stability considerations as given in [1] the temperature profile was found to be extremely significant. Two temperature profiles that were used are the following:

$$T = T_0 \operatorname{erf}\left(\frac{y\sqrt{3}}{\delta}\right), \quad y \geq 0, \tag{1.1}$$

$$T = 0 \quad \text{for} \quad 0 \leq y \leq \delta/(n+1),$$

$$T = \frac{T_0}{2}\left\{1 - \cos \pi \frac{y(n+1) - \delta}{n\delta}\right\} \quad \text{for} \quad \delta/(n+1) \leq y \leq \delta \tag{1.2}$$

$$T = T_0 \quad \text{for} \quad \delta \leq y,$$

where $\text{erf}(x) = [2/\sqrt{(\pi)}] \int_0^x e^{-u^2} du$; δ is a length scale which increases as a certain function of time and is a measure of the depth in which an appreciable temperature gradient has been formed. Here, as in [1], δ is used as the "load parameter," and n is taken equal to 1/2.

The present analysis considers the temperature profiles given by eqns (1.1) and (1.2). It will be shown that for temperature profile (1.1), and when three interacting cracks are considered, then cracks do not snap closed; this is in contrast to the case where only two interacting cracks are used, as in [1]. Instead, all cracks remain open with some growing at the expense of others. For temperature profile (1.2), on the other hand, the inclusion of the third crack does not change the results previously obtained by Nemat-Nasser *et al.*[1].

2. STABILITY ANALYSIS

The stability analysis for the case of an elastic, homogeneous, isotropic half space $y \geq 0$, having an infinite array of initially equally spaced cracks is considered. It is useful to examine the cases of noninteracting cracks, two interacting cracks, and three interacting cracks sequentially so that the difference in the three situations can be made clear.

Noninteracting cracks. If there are no interactions between cracks, then we can consider the unit cell as given by Fig. 1(a). Let the total elastic energy contained in the body per unit thickness per unit cell be

$$\mathscr{E} = \mathscr{E}(h, \delta) \tag{2.1}$$

and let

$$S = 2\gamma h \tag{2.2}$$

be the surface energy measured per unit thickness perpendicular to the x,y-plane. The total potential energy is

$$\Pi = \mathscr{E} + S \tag{2.3}$$

and the vanishing of the first variation of Π, for $dh > 0$, defines the equilibrium state given by

$$-\frac{\partial \mathscr{E}}{\partial h} \equiv G = 2\gamma \equiv G_c \tag{2.4}$$

where G is the energy release rate whose critical value is denoted by G_c; note that because of the assumed fracture criterion, we must have $G \leq G_c$. The stress intensity factor, K, is related to G by

$$G = \frac{1-\nu^2}{E} K^2.$$

The stability of the equilibrium state is guaranteed when the second variation of Π is positive for admissible variation of crack length dh, i.e. when

$$\partial K/\partial h < 0 \tag{2.5}$$

for $dh > 0$.

Two interacting cracks (see [1]). For this case, which is applicable to Fig. 1(b), let $G_1 = G_2 = G_c$ and consider the case when $dh_2 > 0$. Note that here $G_i = G_i(h_1, h_2, \delta)$. The total potential energy is again given by eqn (2.3) but in this case we have

$$\mathscr{E} = \mathscr{E}(h_1, h_2, \delta), \quad S = 2\gamma(h_1 + h_2). \tag{2.6}$$

The equilibrium state is defined by setting equal to zero (for fixed δ) the first variation of Π for $dh_i > 0$, which gives $-\partial \mathscr{E}/\partial h_i \equiv G_i = G_c$. The stability of this state can be investigated by

consideration of the second variation of Π for admissible variations, $dh_i \geq 0$; this leads to

$$\frac{\partial^2 \mathscr{E}}{\partial h_i \partial h_j} dh_i dh_j \begin{cases} >0 & \text{stable} \\ =0 & \text{critical, for all } dh_i \geq 0 \\ <0 & \text{unstable} \end{cases} \tag{2.7}$$

where repeated indices are summed for $i,j = 1,2$. With $dh_2 > 0$ set $z = dh_1/dh_2$ and obtain from (2.7)

$$\frac{\partial G_1}{\partial h_1} z^2 + 2\frac{\partial G_1}{\partial h_2} z + \frac{\partial G_2}{\partial h_2} \begin{cases} <0 & \text{stable} \\ =0 & \text{critical, for all } z \geq 0 \\ >0 & \text{unstable.} \end{cases} \tag{2.8}$$

As has been shown in [1] $\partial G_1/\partial h_2 = \partial G_2/\partial h_1 < 0$ for the present problem and therefore for the equilibrium state $G_1 = G_2 = G_c$ to be unstable it is both necessary and sufficient that

$$\partial G_1/\partial h_1 > 0 \quad \text{or} \quad \partial G_2/\partial h_2 > 0. \tag{2.9}$$

Moreover, the equilibrium state is stable if and only if

$$\frac{\partial G_1}{\partial h_1} < 0 \quad \text{and} \quad \frac{\partial G_2}{\partial h_2} < 0. \tag{2.10}$$

The critical condition is obtained from

$$\frac{\partial G_1}{\partial h_1} = 0 \quad \text{or} \quad \frac{\partial G_2}{\partial h_2} = 0. \tag{2.11}$$

In this case one crack stops growing, while the other crack grows at a faster rate. Critical condition (2.11) has been used for stability in [1]. Figure 2 (taken from [1]) describes the results of such an analysis for the temperature profile given by eqn (1.1). Note that for this figure $\Delta = \delta/b$ is the dimensionless load parameter, $a_2 = h_2/b$ is the dimensionless length, and the dimensionless critical stress intensity factor $N_c = K_c/\sqrt{(2\pi)}\hat{\beta}T_0\sqrt{(b)}$ has the value, $N_c = 0.15$, where $\hat{\beta} = 3\hat{\alpha}E/(1-2\nu)$ and $\hat{\alpha}$ is the coefficient of thermal expansion. Along line AB the cracks

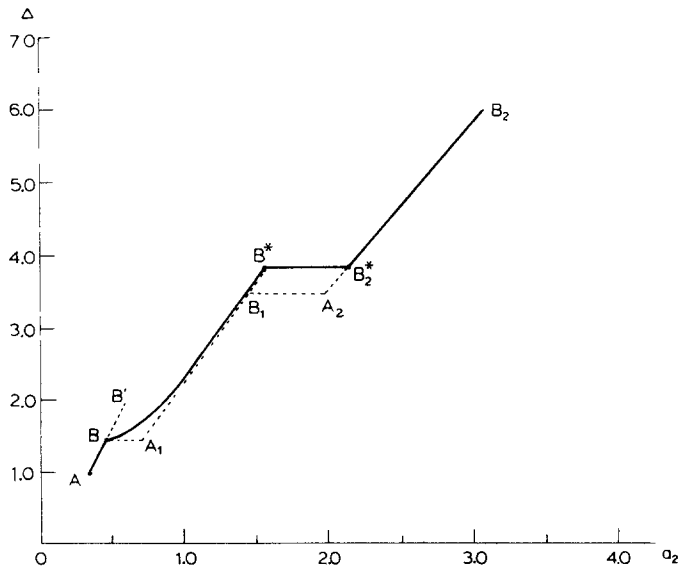

Fig. 2. After Ref. [1] (Fig. 10). Variations in crack lengths and crack spacing as functions of the load parameter Δ for temperature profile (1.1).

grow equally with an increase in the load parameter, Δ. For states corresponding to this portion of the curve we have $\partial N_1/\partial a_1 = \partial N_2/\partial a_2 \leq 0$ (the equality corresponds to the point B only) and therefore all states on this branch are stable, except for point B which is critical. On the other hand for the portion BB' we have $\partial N_1/\partial a_1 = \partial N_2/\partial a_2 > 0$ and therefore all states between B and B' are unstable. It should be noted that if the unit cell given in Fig. 1(a) is used (noninteracting crack case) then it would be concluded that the branch BB' would be stable, since then $\partial N/\partial a < 0$. It is thus only through the consideration of interacting cracks (Fig. 1b), that the critical state at B can be identified.

After point B, crack 1 ceases to grow, while crack 2 continues to extend, as Δ is increased (for proof, see [1]). This process continues until the point B^* is reached. At this point N_1 becomes zero, and after this point it becomes negative. Curve A_1B_1 in Fig. 2 represents the stable states for a system of cracks with spacing $2b$, and curve A_2B_2 is for the stable states with crack spacing equal to $4b$. Now, after point B^* the only possible state is along curve A_2B_2, which represents a quadrupling of the crack spacing. Hence, if only two interacting cracks are considered, then at state B^* not only those cracks which had ceased growing along branch BB^*, but also every other of the remaining cracks would close with a further increase of Δ. In [1] the question was raised whether this phenomenon actually occurs or whether it also represents a constrained stability due to the fact that three interacting cracks have not been considered. This latter case will now be discussed.

Three interacting cracks. This case is applicable to Fig. 1(c). For given crack lengths h_1, h_2 and h_3, let the total elastic energy contained in the body per unit thickness per unit cell be denoted by $\mathscr{E} = \mathscr{E}(h_1, h_2, h_3, \delta)$. Here we note that h_1 remains fixed ($dh_1 = 0$) because

$$0 < G_1 = -\partial\mathscr{E}/\partial h_1 < G_c. \tag{2.12}$$

For the three crack case shown in Fig. 1(c)

$$G_1 = \frac{1-\nu^2}{E}(K_{I1}^2 + K_{II1}^2) \tag{2.13}$$

$$G_2 = \frac{1-\nu^2}{E} K_{I2}^2 \tag{2.14}$$

$$G_3 = \frac{1-\nu^2}{E} K_{I3}^2 \tag{2.15}$$

where K_{I1}, K_{II1} are Mode I and II stress intensity factors for crack 1 and K_{I2} and K_{I3} are, respectively, the Mode I stress intensity factors for cracks 2 and 3. Since crack 1 is stationary, the stability analysis will be concerned only with cracks 2 and 3. The equilibrium state is defined by setting equal to zero (for fixed δ) the first variation of the total potential energy given by (2.3) where $\mathscr{E}$ and S now depend on h_1, h_2 and h_3. This results in, for $dh_i > 0$, $i = 2, 3$ and $dh_1 = 0$,

$$-\partial\mathscr{E}/\partial h_i = G_c, \quad i = 2, 3. \tag{2.16}$$

The stability of this equilibrium can be investigated by considering the sign of the second variation of the total potential energy for admissible variations $dh_i \geq 0$, $i = 2, 3$. Suppose that $dh_2 > 0$, and set $z = dh_3/dh_2$, where $z \geq 0$. Stability conditions are then given by

$$F \equiv \frac{\partial G_3}{\partial h_3} z^2 + 2\frac{\partial G_3}{\partial h_2} z + \frac{\partial G_2}{\partial h_2} \begin{cases} < 0 & \text{stable} \\ = 0 & \text{critical,} \quad z \geq 0 \\ > 0 & \text{unstable.} \end{cases} \tag{2.17}$$

Here we also have

$$\frac{\partial G_3}{\partial h_2} = \frac{\partial G_2}{\partial h_3} < 0. \tag{2.18}$$

Relation (2.18) holds if we recall that crack 1 remains stationary and a corresponding extension of, say, crack 2 results in a relaxation of the elastic stress field around crack 3 causing the incremental reduction in the magnitude of K_{I3} (see [1]). Thus, for the case when $K_{I2} = K_{I3} = K_c$, F will be strictly positive if and only if

$$\frac{\partial G_2}{\partial h_2} < 0 \quad \text{and} \quad \frac{\partial G_3}{\partial h_3} < 0. \tag{2.19}$$

On the other hand F ceases to be positive if and only if

$$\frac{\partial G_2}{\partial h_2} > 0 \quad \text{or} \quad \frac{\partial G_3}{\partial h_3} > 0. \tag{2.20}$$

Therefore, we conclude that for a system of three interacting cracks, if one of the cracks (crack 1) is stationary, then cracks 2 and 3 grow at equal rates ($h_2 = h_3$) with increasing δ, provided that $\partial G_2/\partial h_2 = \partial G_3/\partial h_3 < 0$. If a state is reached at which $\partial G_2/\partial h_2 = \partial G_3/\partial h_3 = 0$, then the growth regime becomes critical. After this state, crack 3, say, stops growing, while crack 2 continues to extend with increasing δ. In the numerical example, this occurs at a state corresponding to a point close to B_1 in Fig. 2. (See Fig. 4.)

Numerical results. Some of the numerical results for the case of three interacting cracks (Fig. 1c), will now be reported. The basic equations used for the required analysis are presented in Section 3 which is self-contained.

We have obtained results for both temperature profiles, (1.1) and (1.2), with $N_c = 0.15$.

For temperature profile (1.2), our results for three interacting cracks in a unit cell are essentially identical to those for two interacting cracks given in [1]. Figure 3 is taken from [1]. For states corresponding to points on branch AB in Fig. 3 the cracks grow at an equal rate with increasing δ. At the state associated with point B, every other crack stops growing. At the state associated with point B^*, N_1 becomes zero. At this state those cracks which had ceased to grow will snap closed (this has been proved in [1]) while the remaining cracks jump to a finitely longer length corresponding to point $B\dagger$ in Fig. 3. For states associated with branch $B\dagger B_1$, crack 1 is closed but crack 2 extends with increasing δ.

In [1] it has been assumed that crack 1 remains completely *inactive* after state $B\dagger$, as if it had never existed. In our present calculation we have relaxed this constraint, allowing crack 1 to remain active in shear after state $B\dagger$ is reached. Hence, for the three interacting cracks

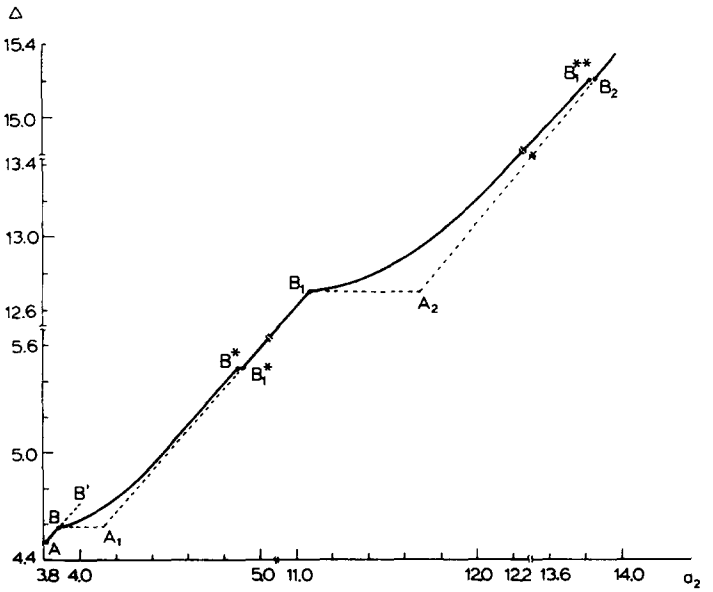

Fig. 3. After Ref. [1] (Fig. 8). Variations in crack lengths and crack spacing as functions of the load parameter Δ for temperature profile eqn (1.2).

considered here, crack closure is assumed to mean that the normal displacements (which tend to open the crack) are zero, but that the tangential (shearing) displacements are not necessarily zero. However, our results are not altered noticeably by the inclusion of the shear displacement effects for the temperature profile (1.2).

For the temperature profile (1.1) consideration of the three interacting cracks leads to new results which are qualitatively different than those given in [1]. We shall summarize these new results next.

(a) Cracks grow at equal rates until a critical state, corresponding to point B in Fig. 4, is reached. At this point every other crack ceases to grow, while the remaining cracks grow at a faster rate with increasing δ. This corresponds to branch BB_1 in Fig. 4 (the solid curve), on which crack 1 has a constant length equal to that associated with point B, i.e. $a_1 = 0.459$.

(b) At the state corresponding to point B_1 (which is located below point $B\dagger$ on the branch $BB_1B\dagger$), every other of those cracks which have continued to grow with increasing δ (along branch BB_1) stop growing, while the remaining cracks continue to extend with increasing δ. After this state the unit cell will be as shown in Fig. 1(c), where cracks 1 and 3 are stationary (with $a_1 = 0.459$ and $a_3 = 1.442$), while crack 2 increases with increasing δ. The values of the energy release rates G_1 and G_2 (at cracks 1 and 2, respectively) remain less than G_c for states corresponding to the branch B_1B_2, but do not become zero. Moreover, the Mode I stress intensity factors K_{I1} and K_{I3} never cease to be positive for the three crack system, which indicates that no crack closure takes place for this case. We therefore see that the analysis presented in [1] for two interacting cracks represents a constrained stability analysis in the sense that branch $B_1B\dagger^*$, which has been regarded to represent stable states for the two crack system, actually corresponds to unstable states when the unit cell having three cracks (Fig. 1c) is considered.

At point B_1 in Fig. 4, $a_1 = 0.459$, and $a_2 = a_3 = 1.442$. Points on the *solid* curve B_1B_2 correspond to states for which $a_1 = 0.459$, $a_3 = 1.442$, and a_2 is increasing with Δ. Points on the *dashed* curve B_1B_2, on the other hand, correspond to a unit cell in which crack 1 is assumed to not exist (to be inactive in shear as well as in normal displacement; i.e. crack 1 is assumed to be glued back together). As is seen by comparing the solid and the dashed curves B_1B_2, the inclusion of crack 1 changes the results only very slightly.

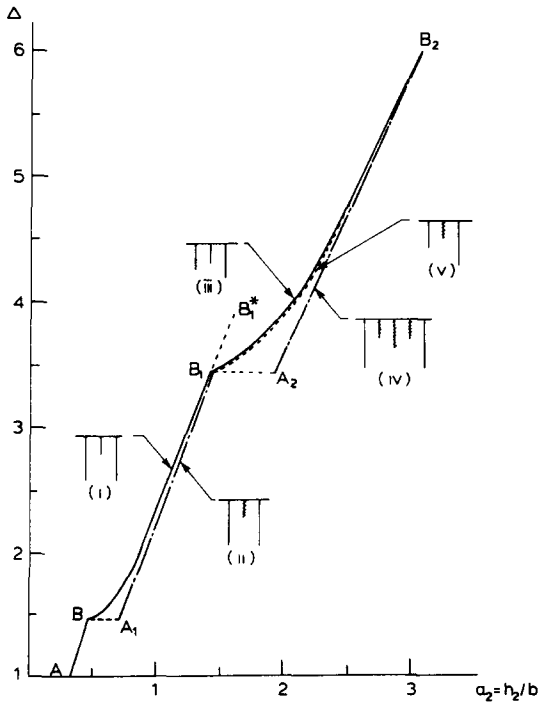

Fig. 4. Variations in crack lengths and crack spacing as functions of the load parameter Δ for temperature profile eqn (1.1). Unit cells used to obtain the indicated portions of the growth curves are denoted by inserts (i)–(v) as discussed in text (Section 2, Numerical results).

The dash-dot curve A_2B_2 in Fig. 4 is obtained for noninteracting cracks with spacing equal to $4b$, and the dash-dot curve A_1B_1 is for noninteracting cracks with spacing equal to $2b$. Since point B_1 on the solid curve BB_1 is essentially the same as that on the dash-dot curve A_1B_1, which can be obtained with considerably less effort, and also since the same comments apply to point B_2 and curve A_2B_2, we see that curves AB, A_1B_1, A_2B_2, etc. are sufficient to give the essential features of the growth regime of interacting straight edge cracks considered in this study. After these curves are obtained, points B, B_1, B_2, etc. can be established by a stability analysis which involves only two interacting cracks.

Various curves in Fig. 4 are identified by the inserts given therein. Insert (i) (for curve BB_1) represents the case where every other crack has ceased to grow while the remaining cracks continue to grow at a faster rate; insert (ii) (for curve A_1B_1) shows the results corresponding to the solution for the case where every other crack is removed; insert (iii) (for curve B_1B_2) shows the results corresponding to the case where two cracks have ceased to grow, while the remaining crack in the unit cell continues to grow at a faster rate. Insert (v) (for curve B_1B_2, dashed) shows the same result as for (iii) but with the central crack assumed to have been removed; and insert (iv) (for curve A_2B_2) gives the result for the crack array with a spacing of $4b$.

3. ANALYSIS FOR THREE INTERACTING CRACKS

We shall now formulate the plane problem of a half-space weakened by a system of equally spaced parallel cracks whose unit cell is given by alternate lengths h_1, h_2 and h_3 (Fig. 1c). Let the crack spacing be b, and let the cracks be opened by a nonuniform temperature distribution (cooling) given by eqn (1.1). The boundary conditions appropriate to the considered problem are then given as

$$\tau_{xx}(0, y) = -\hat{\beta}T_0[1 - \operatorname{erf}(y\sqrt{(3)}/\delta)] \quad 0 < y < h_1 \tag{3.1}$$

$$\tau_{xy}(0, y) = 0 \quad 0 < y < h_1 \tag{3.2}$$

$$\tau_{xx}(b, y) = -\hat{\beta}T_0[1 - \operatorname{erf}(y\sqrt{(3)}/\delta)] \quad 0 < y < h_2 \tag{3.3}$$

$$\tau_{xy}(b, y) = 0 \quad 0 < y < h_2 \tag{3.4}$$

$$\tau_{xx}(-b, y) = -\hat{\beta}T_0[1 - \operatorname{erf}(y\sqrt{(3)}/\delta)] \quad 0 < y < h_3 \tag{3.5}$$

$$\tau_{xy}(-b, y) = 0 \quad 0 < y < h_3. \tag{3.6}$$

It is convenient to use the representation for the components of the stress tensor for a vertical crack in an elastic half-space given by Keer and Chantaramungkorn[6]. A suitable superposition will allow for the complete representation of the crack array. It can be shown that the crack system constructed from cracks 2 and 3 will be entirely in Mode I while the crack system constructed from crack 1 will involve both Modes I and II. Thus boundary conditions, eqns (3.4) and (3.6), will be automatically satisfied by symmetry. The remaining boundary conditions, eqns (3.1)–(3.3), (3.5) lead to the following system of singular integral equations:

$$\frac{\pi}{2b}\int_0^{h_1} D_1(t)G_1\left(\frac{\pi t}{2b}, \frac{\pi y}{2b}\right)dt + \frac{\pi}{4b}\int_0^{h_2} D_2(t)G_2\left(\frac{\pi t}{2b}, \frac{\pi y}{2b}\right)dt + \frac{\pi}{4b}\int_0^{h_3} D_3(t)G_2\left(\frac{\pi t}{2b}, \frac{\pi y}{2b}\right)dt = -\lambda T_0\left[1 - \operatorname{erf}\left(\frac{y\sqrt{3}}{\delta}\right)\right] \quad 0 < y < h_1 \tag{3.7}$$

$$\frac{\pi}{2b}\int_0^{h_1} C_1(t)G_3\left(\frac{\pi t}{2b}, \frac{\pi y}{2b}\right)dt + \frac{\pi}{4b}\int_0^{h_2} D_2(t)G_4\left(\frac{\pi t}{2b}, \frac{\pi y}{2b}\right)dt - \frac{\pi}{4b}\int_0^{h_3} D_3(t)G_4\left(\frac{\pi t}{2b}, \frac{\pi y}{2b}\right)dt = 0 \quad 0 < y < h_1 \tag{3.8}$$

$$\frac{\pi}{2b}\int_0^{h_1} C_1(t)G_5\left(\frac{\pi t}{2b}, \frac{\pi y}{2b}\right)dt + \frac{\pi}{2b}\int_0^{h_1} D_1(t)G_2\left(\frac{\pi t}{2b}, \frac{\pi y}{2b}\right)dt + \frac{\pi}{4b}\int_0^{h_2} D_2(t)G_1\left(\frac{\pi t}{4b}, \frac{\pi y}{4b}\right)dt + \frac{\pi}{4b}\int_0^{h_3} D_3(t)G_2\left(\frac{\pi t}{4b}, \frac{\pi y}{4b}\right)dt = -\lambda T_0\left[1 - \operatorname{erf}\left(\frac{y\sqrt{3}}{\delta}\right)\right] \quad 0 < y < h_2 \tag{3.9}$$

$$-\frac{\pi}{2b}\int_0^{h_1} C_1(t)G_5\left(\frac{\pi t}{2b},\frac{\pi y}{2b}\right)dt+\frac{\pi}{2b}\int_0^{h_1} D_1(t)G_2\left(\frac{\pi t}{2b},\frac{\pi y}{2b}\right)dt+\frac{\pi}{4b}\int_0^{h_2} D_2(t)G_2\left(\frac{\pi t}{4b},\frac{\pi y}{4b}\right)dt$$
$$+\frac{\pi}{4b}\int_0^{h_3} D_3(t)G_1\left(\frac{\pi t}{4b},\frac{\pi y}{4b}\right)dt=-\lambda T_0\left[1-\operatorname{erf}\left(\frac{y\sqrt{3}}{\delta}\right)\right]\quad 0<y<h_3 \tag{3.10}$$

where $\lambda=4\pi\hat{\beta}(1-\nu)(1+\nu)/E$. The functions $C_1(t)$, $D_1(t)$, $D_2(t)$ and $D_3(t)$ represent appropriate dislocation densities and the kernels $G_1(t, y),\ldots G_5(t, y)$ are given by

$$G_1(t,y)=2\coth(y+t)-(y+3t)\operatorname{cosech}^2(y+t)+4ty-\operatorname{cosech}^2(y+t)\coth(y+t)$$
$$-2\coth(y-t)+(y-t)\operatorname{cosech}^2(y-t) \tag{3.11}$$

$$G_2(t,y)=2\tanh(y+t)+(y+3t)\operatorname{sech}^2(y+t)-4ty\operatorname{sech}^2(y+t)\tanh(y+t)$$
$$-2\tanh(y-t)-(y-t)\operatorname{sech}^2(y-t) \tag{3.12}$$

$$G_3(t,y)=(y-t)\operatorname{cosech}(y+t)\coth(y+t)+2ty\operatorname{cosech}(y+t)[2\coth^2(y+t)-1]$$
$$-(y-t)\operatorname{cosech}(y-t)\coth(y-t) \tag{3.13}$$

$$G_4(t,y)=\operatorname{sech}(y+t)-(y+t)\operatorname{sech}(y+t)\tanh(y+t)+2ty\operatorname{sech}(y+t)$$
$$\times[2\tanh^2(y+t)-1]-\operatorname{sech}(y-t)+(y-t)\operatorname{sech}(y-t)\tanh(y-t) \tag{3.14}$$

$$G_5(t,y)=-\operatorname{sech}(y+t)+(y-3t)\operatorname{sech}(y+t)\tanh(y+t)+2ty\operatorname{sech}(y+t)$$
$$\times[2\tanh^2(y+t)-1]+\operatorname{sech}(y-t)-(y-t)\operatorname{sech}(y-t)\tanh(y-t). \tag{3.15}$$

The representation of eqns (3.11)–(3.15) in their series form and their summation is given in the Appendix, eqns (A1)–(A5).

The intervals $(0, h_i)$, $i=1,2,3$ are normalized by appropriately changing to variables $s=t/h_i$, $r=y/h_i$ for $0<t,\ y<h_i$, and by setting

$$C_1(t)=2\lambda T_0A_1(s)/\pi(1-s^2)^{1/2},\quad A_1(s)=A_1(-s),\quad (0<s<1) \tag{3.16}$$

$$D_i(t)=2\lambda T_0B_i(s)/\pi(1-s^2)^{1/2},\quad B_i(s)=B_i(-s),\quad i=1,2,3,\quad (0<s<1) \tag{3.17}$$

which allows for the definition of A_1, B_i in the interval $|s|<1$. (See e.g. Gupta and Erdogan[4].) By using (3.16) and (3.17) and introducing the nondimensional quantities

$$a_1=h_1/b,\quad a_2=h_2/b,\quad a_3=h_3/b,\quad \Delta=\delta/b, \tag{3.18}$$

we can rewrite the integral equations (3.7)–(3.10) in the form

$$\frac{1}{2}\left\{\int_{-1}^{1}\frac{B_1(s)}{(1-s^2)^{1/2}}a_1G_1\left(\frac{\pi a_1|s|}{2},\frac{\pi a_1r}{2}\right)ds+\frac{1}{2}\int_{-1}^{1}\frac{B_2(s)}{(1-s^2)^{1/2}}a_2G_2\left(\frac{\pi a_2|s|}{2},\frac{\pi a_1r}{2}\right)ds\right.$$
$$\left.+\frac{1}{2}\int_{-1}^{1}\frac{B_3(s)}{(1-s^2)^{1/2}}a_3G_2\left(\frac{\pi a_3|s|}{2},\frac{\pi a_1r}{2}\right)ds\right\}=-\left[1-\operatorname{erf}\left(\frac{\sqrt{(3)}a_1r}{\Delta}\right)\right]\quad 0<r<1 \tag{3.19}$$

$$\frac{1}{2}\left\{\int_{-1}^{1}\frac{A_1(s)}{(1-s^2)^{1/2}}a_1G_3\left(\frac{\pi a_1|s|}{2},\frac{\pi a_1r}{2}\right)ds+\frac{1}{2}\int_{-1}^{1}\frac{B_2(s)}{(1-s^2)^{1/2}}a_2G_4\left(\frac{\pi a_2|s|}{2},\frac{\pi a_1r}{2}\right)ds\right.$$
$$\left.-\frac{1}{2}\int_{-1}^{1}\frac{B_3(s)}{(1-s^2)^{1/2}}a_3G_4\left(\frac{\pi a_3|s|}{2},\frac{\pi a_1r}{2}\right)ds\right\}=0\quad 0<r<1 \tag{3.20}$$

$$\frac{1}{2}\left\{\int_{-1}^{1}\frac{A_1(s)}{(1-s^2)^{1/2}}a_1G_5\left(\frac{\pi a_1|s|}{2},\frac{\pi a_2r}{2}\right)ds+\int_{-1}^{1}\frac{B_1(s)}{(1-s^2)^{1/2}}a_1G_2\left(\frac{\pi a_1|s|}{2},\frac{\pi a_2r}{2}\right)ds\right.$$
$$\left.+\frac{1}{2}\int_{-1}^{1}\frac{B_2(s)}{(1-s^2)^{1/2}}a_2G_1\left(\frac{\pi a_2|s|}{4},\frac{\pi a_2r}{4}\right)ds+\frac{1}{2}\int_{-1}^{1}\frac{B_3(s)}{(1-s^2)^{1/2}}a_3G_2\left(\frac{\pi a_3|s|}{4},\frac{\pi a_2r}{4}\right)ds\right\}$$
$$=-\left[1-\operatorname{erf}\left(\frac{\sqrt{(3)}a_2r}{\Delta}\right)\right]\quad 0<r<1 \tag{3.21}$$

$$\frac{1}{2}\left\{-\int_{-1}^{1}\frac{A_1(s)}{(1-s^2)^{1/2}}a_1G_5\left(\frac{\pi a_1|s|}{2},\frac{\pi a_3 r}{2}\right)ds+\int_{-1}^{1}\frac{B_1(s)}{(1-s^2)^{1/2}}a_1G_2\left(\frac{\pi a_1|s|}{2},\frac{\pi a_3 r}{2}\right)ds\right.$$
$$+\frac{1}{2}\int_{-1}^{1}\frac{B_2(s)}{(1-s^2)^{1/2}}a_2G_2\left(\frac{\pi a_2|s|}{4},\frac{\pi a_3 r}{4}\right)ds+\frac{1}{2}\int_{-1}^{1}\frac{B_3(s)}{(1-s^2)^{1/2}}a_3G_1\left(\frac{\pi a_3|s|}{4},\frac{\pi a_3 r}{4}\right)ds\Bigg\}$$
$$=-\left[1-\operatorname{erf}\left(\frac{\sqrt{(3)}a_3 r}{\Delta}\right)\right]\quad 0<r<1. \tag{3.22}$$

Equations (3.18)–(3.22) can be put into the form of simultaneous, algebraic equations by the method described in Gupta and Erdogan[7] and by Erdogan *et al.*[8] as follows:

$$\sum_{i=1}^{n_1}c_1B_1(s_i)a_1G_1(t_{1i},y_{1p})+\frac{1}{2}\sum_{j=1}^{n_2}c_2B_2(s_i)a_2G_2(t_{2j},y_{1p})$$
$$+\frac{1}{2}\sum_{k=1}^{n_3}c_3B_3(s_k)a_3G_2(t_{3k},y_{1p})=-\left[1-\operatorname{erf}\left(\frac{2\sqrt{3}}{\pi\Delta}y_{1p}\right)\right]\quad p=1,2,\ldots n_1 \tag{3.23}$$

$$\sum_{i=1}^{n_1}c_1A_1(s_i)a_1G_3(t_{1i},y_{1p})+\frac{1}{2}\sum_{j=1}^{n_2}c_2B_2(s_j)a_2G_4(t_{2j},y_{1p})$$
$$-\frac{1}{2}\sum_{k=1}^{n_3}c_3B_3(s_k)a_3G_4(t_{3k},y_{1p})=0\quad p=1,2,\ldots n_1 \tag{3.24}$$

$$\sum_{i=1}^{n_1}c_1A_1(s_i)a_1G_5(t_{1i},y_{2p})+\sum_{i=1}^{n_1}c_1B_1(s_i)a_1G_2(t_{1i},y_{2p})+\frac{1}{2}\sum_{j=1}^{n_2}c_2B_2(s_j)a_2G_1\left(\frac{t_{2j}}{2},\frac{y_{2p}}{2}\right)$$
$$+\frac{1}{2}\sum_{k=1}^{n_3}c_3B_3(s_k)a_3G_2\left(\frac{t_{3k}}{2},\frac{y_{2p}}{2}\right)=-\left[1-\operatorname{erf}\left(\frac{2\sqrt{3}}{\pi\Delta}y_{2p}\right)\right]\quad p=1,2,\ldots n_2 \tag{3.25}$$

$$-\sum_{i=1}^{n_1}c_1A_1(s_i)a_1G_5(t_{1i},y_{3p})+\sum_{i=1}^{n_1}c_1B_1(s_i)a_1G_2(t_{1i},y_{3p})+\frac{1}{2}\sum_{j=1}^{n_2}c_2B_2(s_j)a_2G_2\left(\frac{t_{2j}}{2},\frac{y_{3p}}{2}\right)$$
$$+\frac{1}{2}\sum_{k=1}^{n_3}c_3B_3(s_k)a_3G_1\left(\frac{t_{3k}}{2},\frac{y_{3p}}{2}\right)=-\left[1-\operatorname{erf}\left(\frac{2\sqrt{3}}{\pi\Delta}y_{3p}\right)\right]\quad p=1,2,\ldots n_3 \tag{3.26}$$

where n_1, n_2 and n_3 are the numbers of integration points in cracks h_1, h_2 and h_3, respectively. Furthermore

$$c_i=\pi/(2n_i+1),\quad i=1,2,3 \tag{3.27}$$

$$s_i=\cos\left(\frac{2i-1}{2n_1+1}\frac{\pi}{2}\right),\quad s_j=\cos\left(\frac{2j-1}{2n_2+1}\frac{\pi}{2}\right),\quad s_k=\cos\left(\frac{2k-1}{2n_3+1}\frac{\pi}{2}\right) \tag{3.28}$$

$$t_{1i}=\pi a_1 s_i/2,\quad t_{2j}=\pi a_2 s_j/2,\quad t_{3k}=\pi a_3 s_k/2 \tag{3.29}$$

$$y_{1p}=\frac{\pi a_1}{2}\cos\left(\frac{p\pi}{2n_1+1}\right),\quad y_{2p}=\frac{\pi a_2}{2}\cos\left(\frac{p\pi}{2n_2+1}\right),\quad y_{3p}=\frac{\pi a_3}{2}\cos\left(\frac{p\pi}{2n_3+1}\right). \tag{3.30}$$

Let N_{II1} denote the Mode II stress-intensity factor at the crack tip $(0, a_1)$ and let N_{I1}, N_{I2} and N_{I3} denote the Mode I stress-intensity factors at the crack tips $(0, a_1)$, (b, a_2) and $(-b, a_3)$, respectively. Then, the stress-intensity factors can be obtained directly from the appropriate dislocation densities and are defined as follows:

$$N_{II1}=\lim_{y\to a_1^+}\sqrt{(y-a_1)}\tau_{xy}(0,y)=-\sqrt{(2a_1)}A_1(1) \tag{3.31}$$

$$N_{I1}=\lim_{y\to a_1^+}\sqrt{(y-a_1)}\tau_{xx}(0,y)=-\sqrt{(2a_1)}B_1(1) \tag{3.32}$$

$$N_{I2}=\lim_{y\to a_2^+}\sqrt{(y-a_2)}\tau_{xy}(b,y)=-\sqrt{(2a_2)}B_2(1) \tag{3.33}$$

$$N_{I3}=\lim_{y\to a_3^+}\sqrt{(y-a_3)}\tau_{xx}(-b,y)=-\sqrt{(2a_3)}B_3(1). \tag{3.34}$$

The values of $A_1(1)$, $B_1(1)$, $B_2(1)$ and $B_3(1)$ can be obtained by using the method described in Krenk[9] as

$$A_1(1)=\frac{-2}{2n_1+1}\left\{\sum_{i=1}^{n_1}(-1)^i A_1(s_i)\operatorname{cosec}\left(\frac{2i-1}{2n_1+1}\frac{\pi}{2}\right)-(-1)^{n_1}\frac{A_1(0)}{2}\right\} \tag{3.35}$$

$$B_1(1)=\frac{-2}{2n_1+1}\left\{\sum_{i=1}^{n_1}(-1)^i B_1(s_i)\operatorname{cosec}\left(\frac{2i-1}{2n_1+1}\frac{\pi}{2}\right)-(-1)^{n_1}\frac{B_1(0)}{2}\right\} \tag{3.36}$$

$$B_2(1)=\frac{-2}{2n_2+1}\left\{\sum_{j=1}^{n_2}(-1)^j B_2(s_j)\operatorname{cosec}\left(\frac{2j-1}{2n_2+1}\frac{\pi}{2}\right)-(-1)^{n_2}\frac{B_2(0)}{2}\right\} \tag{3.37}$$

$$B_3(1)=\frac{-2}{2n_3+1}\left\{\sum_{k=1}^{n_3}(-1)^k B_3(s_k)\operatorname{cosec}\left(\frac{2k-1}{2n_3+1}\frac{\pi}{2}\right)-(-1)^{n_3}\frac{B_3(0)}{2}\right\}. \tag{3.38}$$

To adequately discuss the stability of the crack system it is necessary to obtain derivatives of the stress-intensity factors N_{III}, $N_{\mathrm{II}1}$, $N_{\mathrm{II}2}$ and $N_{\mathrm{II}3}$ with respect to the lengths a_1, a_2 and a_3; they are given by

$$\frac{\partial N_{\mathrm{III}}}{\partial a_1}=\frac{N_{\mathrm{III}}}{2a_1}-\sqrt{(2a_1)}\frac{\partial A_1(1)}{\partial a_1} \tag{3.39}$$

$$\frac{\partial N_{\mathrm{II}1}}{\partial a_1}=\frac{N_{\mathrm{II}1}}{2a_1}-\sqrt{(2a_1)}\frac{\partial B_1(1)}{\partial a_1} \tag{3.40}$$

$$\frac{\partial N_{\mathrm{II}2}}{\partial a_1}=-\sqrt{(2a_2)}\frac{\partial B_2(1)}{\partial a_1} \tag{3.41}$$

$$\frac{\partial N_{\mathrm{II}3}}{\partial a_1}=-\sqrt{(2a_3)}\frac{\partial B_3(1)}{\partial a_1}. \tag{3.42}$$

The values of $(\partial A_1(1)/\partial a_1)$, $(\partial B_1(1)/\partial a_1)$, $(\partial B_2(1)/\partial a_1)$ and $(\partial B_3(1)/\partial a_1)$ can be determined by using eqns (3.5)–(3.8), respectively. The derivatives $(\partial A_1(s_i)/\partial a_1)$, $(\partial B_1(s_i)/\partial a_1)$, $(\partial B_2(s_j)/\partial a_1)$ and $(\partial B_3(s_k)/\partial a_1)$ can be found by differentiating eqns (3.23)–(3.26); their form is deduced from

$$\begin{aligned}\sum_{i=1}^{n_1}c_1\frac{\partial B_1(s_i)}{\partial a_1}a_1G_1(t_{1i},y_{1p})+\frac{1}{2}\sum_{j=1}^{n_2}c_2\frac{\partial B_2(s_j)}{\partial a_1}a_2G_2(t_{2j},y_{1p})+\frac{1}{2}\sum_{k=1}^{n_3}c_3\frac{\partial B_3(s_k)}{\partial a_1}a_3G_2(t_{3k},y_{1p})\\ =\frac{2}{a_1\sqrt{\pi}}\left(\frac{2\sqrt{3}}{\pi\Delta}y_{1p}\right)\mathrm{e}^{-((2\sqrt{(3)}/\pi\Delta)y_{1p})^2}-\sum_{i=1}^{n_1}c_1B_1(s_i)L_1(t_{1i},y_{1p})-\frac{1}{2}\sum_{j=1}^{n_2}B_2(s_j)\frac{a_2}{a_1}L_4(t_{2j},y_{1p})\\ -\frac{1}{2}\sum_{k=1}^{n_3}B_3(s_k)\frac{a_3}{a_1}L_4(t_{3k},y_{1p})\quad p=1,2,\ldots n_1\end{aligned} \tag{3.43}$$

$$\begin{aligned}\sum_{i=1}^{n_1}c_1\frac{\partial A_1(s_i)}{\partial a_1}a_1G_3(t_{1i},y_{1p})+\frac{1}{2}\sum_{j=1}^{n_2}c_2B_2(s_j)a_2G_4(t_{2j},y_{1p})-\frac{1}{2}\sum_{k=1}^{n_3}c_3B_3(s_k)a_3G_4(t_{3k},y_{1p})\\ =-\frac{1}{2}\sum_{i=1}^{n_1}c_1A_1(s_i)L_2(t_{1i},y_{1p})-\frac{1}{2}\sum_{j=1}^{n_2}c_2B_2(s_j)\frac{a_2}{a_1}L_6(t_{2j},y_{1p})\\ +\frac{1}{2}\sum_{k=1}^{n_3}B_3(s_k)\frac{a_3}{a_2}L_6(t_{3k},y_{1p})\quad p=1,2,\ldots n_1\end{aligned} \tag{3.44}$$

$$\begin{aligned}\sum_{i=1}^{n_1}c_1\frac{\partial A_1(s_i)}{\partial a_1}a_1G_5(t_{1i},y_{2p})+\sum_{i=1}^{n_1}c_1\frac{\partial B_1(s_i)}{\partial a_1}a_1G_2(t_{1i},y_{2p})\\ +\frac{1}{2}\sum_{j=1}^{n_2}c_2\frac{\partial B_2(s_j)}{\partial a_1}a_2G_1\left(\frac{t_{2j}}{2},\frac{y_{2p}}{2}\right)+\frac{1}{2}\sum_{k=1}^{n_3}c_3\frac{\partial B_3}{\partial a_1}a_3G_2\left(\frac{t_{3k}}{2},\frac{y_{2p}}{2}\right)\\ =-\sum_{i=1}^{n_1}c_1A_1(s_i)L_7(t_{1i},y_{2p})-\sum_{i=1}^{n_1}c_1B_1(s_i)L_3(t_{1i},y_{2p})\quad p=1,2,\ldots n_2\end{aligned} \tag{3.45}$$

$$-\sum_{i=1}^{n_1} c_1 \frac{\partial A_1(s_i)}{\partial a_1} a_1 G_5(t_{1i}, y_{3p}) + \sum_{i=1}^{n_1} c_1 \frac{\partial B_1(s_i)}{\partial a_1} a_1 G_2(t_{1i}, y_{3p})$$

$$+\frac{1}{2}\sum_{j=1}^{n_2} c_2 \frac{\partial B_2(s_j)}{\partial a_1} a_2 G_2\left(\frac{t_{2j}}{2}, \frac{y_{3p}}{2}\right) + \frac{1}{2}\sum_{k=1}^{n_3} c_3 \frac{\partial B_3(s_k)}{\partial a_1} a_3 G_1\left(\frac{t_{3k}}{2}, \frac{y_{3p}}{2}\right)$$

$$= \sum_{i=1}^{n_1} c_1 A_1(s_i) L_7(t_{1i}, y_{3p}) - \sum_{i=1}^{n_1} c_1 B_1(s_i) L_3(t_{1i}, y_{3p}) \quad p = 1, 2, \ldots n_3 \tag{3.46}$$

where

$$L_1(at, ay) = a \frac{\partial}{\partial a} G_1(at, ay) \tag{3.47}$$

$$L_2(at, ay) = a \frac{\partial}{\partial a} G_3(at, ay) \tag{3.48}$$

$$L_3(at, by) = a \frac{\partial}{\partial a} G_2(at, by) \tag{3.49}$$

$$L_4(at, by) = b \frac{\partial}{\partial b} G_2(at, by) \tag{3.50}$$

$$L_5(at, by) = a \frac{\partial}{\partial a} G_4(at, by) \tag{3.51}$$

$$L_6(at, by) = b \frac{\partial}{\partial b} G_4(at, by) \tag{3.52}$$

$$L_7(at, by) = a \frac{\partial}{\partial a} G_5(at, by) \tag{3.53}$$

$$L_8(at, by) = b \frac{\partial}{\partial b} G_5(at, by). \tag{3.54}$$

Upon performing the indicated differentiations, eqns (3.47)–(3.54), with the aid of eqns (3.11)–(3.15), we obtain

$$L_1(t, y) = 12t + 2\coth(y+t) - 4(y+2t)\coth^2(y+t) + 2(y^2+10yt+3t^2)\coth(y+t)\operatorname{cosech}^2(y+t)$$
$$- 4yt(y+t)\operatorname{cosech}^2(y+t)[3\coth^2(y+t) - 1] - 2\coth(y-t) + 4(y-t)\coth^2(y-t)$$
$$- 2(y-t)^2\coth(y-t)\operatorname{cosech}^2(y-t) \tag{3.55}$$

$$L_2(t, y) = 2(y-t)\coth(y+t)\operatorname{cosech}(y+t) - (y^2-6yt-t^2)\operatorname{cosech}(y+t)[2\coth^2(y+t) - 1]$$
$$- 2yt(y+t)\operatorname{cosech}(y+t)\coth(y+t)[6\coth^2(y+t) - 5] - 2(y-t)\operatorname{cosech}(y-t)$$
$$\times \coth(y-t) + (y-t)^2\operatorname{cosech}(y-t)[2\coth^2(y-t) - 1] \tag{3.56}$$

$$L_3(t, y) = 12t + 2\tanh(y+t) - (y+8t)\tanh^2(y+t) - t(10y+6t)\tanh(y+t)\operatorname{sech}^2(y+t)$$
$$+ 4yt^2\operatorname{sech}^2(y+t)[3\tanh^2(y+t) - 1] - 2\tanh(y-t) + (y-4t)\tanh^2(y-t)$$
$$- 2t(y-t)\tanh(y-t)\operatorname{sech}^2(y-t) \tag{3.57}$$

$$L_4(t, y) = -3y\tanh^2(y+t) - 2y(y+5t)\tanh(y+t)\operatorname{sech}^2(y+t) + 4y^2t\operatorname{sech}^2(y+t)$$
$$\times[3\tanh^2(y+t) - 1] + 3y\tanh^2(y-t) + 2y(y-t)\tanh(y-t)\operatorname{sech}^2(y-t) \tag{3.58}$$

$$L_5(t, y) = \operatorname{sech}(y+t) - (y+3t)\tanh(y+t)\operatorname{sech}(y+t) + t(5y+t)\operatorname{sech}(y+t)[2\tanh^2(y+t) - 1]$$
$$- 2yt^2\tanh(y+t)\operatorname{sech}(y+t)[6\tanh^2(y+t) - 5] - \operatorname{sech}(y-t)$$
$$+ (y-3t)\operatorname{sech}(y-t)\tanh(y-t) + t(y-t)\operatorname{sech}(y-t)[2\tanh^2(y-t) - 1] \tag{3.59}$$

$$L_6(t, y) = -2y \operatorname{sech}(y+t)\tanh(y+t) + y(y+2t)\operatorname{sech}(y+t)[2\tanh^2(y+t)-1]$$
$$-2y^2 t \operatorname{sech}(y+t)\tanh(y+t)[6\tanh^2(y+t)-5] + 2y\operatorname{sech}(y-t)\tanh(y-t)$$
$$-y(y-t)\operatorname{sech}(y-t)[2\tanh^2(y-t)-1] \tag{3.60}$$

$$L_7(t, y) = -\operatorname{sech}(y+t) + (y-5t)\operatorname{sech}(y+t)\tanh(y+t) + 3t(y+t)\operatorname{sech}(y+t)[2\tanh^2(y+t)-1]$$
$$-2yt^2 \operatorname{sech}(y+t)\tanh(y+t)[6\tanh^2(y+t)-5] + \operatorname{sech}(y-t)$$
$$-(y-3t)\operatorname{sech}(y-t)\tanh(y-t) - t(y-t)\operatorname{sech}(y-t)[2\tanh^2(y-t)-1] \tag{3.61}$$

$$L_8(t, y) = 2y\operatorname{sech}(y+t)\tanh(y+t) - y(y-5t)\operatorname{sech}(y+t)[2\tanh^2(y+t)-1]$$
$$-2y^2 t \operatorname{sech}(y+t)\tanh(y+t)[6\tanh^2(y+t)-5] - 2y\operatorname{sech}(y-t)\tanh(y-t)$$
$$+y(y-t)\operatorname{sech}(y-t)[2\tanh^2(y-t)-1]. \tag{3.62}$$

The derivatives of N_{III}, N_{I1}, N_{I2} and N_{I3} with respect to a_2 are given by

$$\frac{\partial N_{III}}{\partial a_2} = -\sqrt{(2a_1)}\frac{\partial A_1(1)}{\partial a_2} \tag{3.63}$$

$$\frac{\partial N_{I1}}{\partial a_2} = -\sqrt{(2a_1)}\frac{\partial B_1(1)}{\partial a_2} \tag{3.64}$$

$$\frac{\partial N_{I2}}{\partial a_2} = \frac{N_{I2}}{2a_2} - \sqrt{(2a_2)}\frac{\partial B_2(1)}{\partial a_2} \tag{3.65}$$

$$\frac{\partial N_{I3}}{\partial a_2} = -\sqrt{(2a_3)}\frac{\partial B_3(1)}{\partial a_2}. \tag{3.66}$$

The derivatives $(\partial A_1(s_i)/\partial a_2)$, $(\partial B_1(s_i)/\partial a_2)$, $(\partial B_2(s_j)/\partial a_2)$ and $(\partial B_3(s_k)/\partial a_2)$ can be determined from the following system of linear equations:

$$\sum_{i=1}^{n_1} c_1 \frac{\partial B_1(s_i)}{\partial a_2} a_1 G_1(t_{1i}, y_{1p}) + \frac{1}{2}\sum_{j=1}^{n_2} c_2 \frac{\partial B_2(s_j)}{\partial a_2} a_2 G_2(t_{2j}, y_{1p})$$
$$+\frac{1}{2}\sum_{k=1}^{n_3} c_3 \frac{\partial B_3(s_k)}{\partial a_2} a_3 G_2(t_{3k}, y_{1p}) = -\frac{1}{2}\sum_{j=1}^{n_2} c_2 B_2(s_j) L_3(t_{2j}, y_{1p}) \quad p = 1, 2, \ldots n_1 \tag{3.67}$$

$$\sum_{i=1}^{n_1} c_1 \frac{\partial A_1(s_i)}{\partial a_2} a_1 G_3(t_{1i}, y_{1p}) + \frac{1}{2}\sum_{j=1}^{n_2} c_2 \frac{\partial B_2(s_j)}{\partial a_2} a_2 G_4(t_{2j}, y_{1p})$$
$$-\frac{1}{2}\sum_{k=1}^{n_3} c_3 \frac{\partial B_3(s_k)}{\partial a_2} a_3 G_4(t_{3k}, y_{1p}) = -\frac{1}{2}\sum_{j=1}^{n_2} c_2 B_2(s_j) L_5(t_{2j}, y_{1p}) \quad p = 1, 2, \ldots n_1 \tag{3.68}$$

$$\sum_{i=1}^{n_1} c_1 \frac{\partial A_1(s_i)}{\partial a_2} a_1 G_5(t_{1i}, y_{2p}) + \sum_{i=1}^{n_1} c_1 \frac{\partial B_1(s_i)}{\partial a_2} a_1 G_2(t_{1i}, y_{2p})$$
$$+\frac{1}{2}\sum_{j=1}^{n_2} c_2 \frac{\partial B_2(s_j)}{\partial a_2} a_2 G_1\left(\frac{t_{2j}}{2}, \frac{y_{2p}}{2}\right) + \frac{1}{2}\sum_{k=1}^{n_3} c_3 \frac{\partial B_3(s_k)}{\partial a_2} a_3 G_2\left(\frac{t_{3k}}{2}, \frac{y_{2p}}{2}\right)$$
$$= \frac{2}{a_2\sqrt{\pi}}\left(\frac{2\sqrt{3}}{\pi\Delta} y_{2p}\right) e^{-((2\sqrt{(3)}/\pi\Delta)y_{2p})^2} - \sum_{i=1}^{n_1} c_1 A_1(s_i)\frac{a_1}{a_2} L_8(t_{1i}, y_{2p})$$
$$-\sum_{i=1}^{n_1} c_1 B_1(s_i)\frac{a_1}{a_2} L_4(t_{1i}, y_{2p}) - \frac{1}{2}\sum_{j=1}^{n_2} c_2 B_2(s_j) L_1\left(\frac{t_{2j}}{2}, \frac{y_{2p}}{2}\right)$$
$$-\frac{1}{2}\sum_{k=1}^{n_3} c_3 B_3(s_k)\frac{a_3}{a_2} L_4\left(\frac{t_{3k}}{2}, \frac{y_{2p}}{2}\right) \quad p = 1, 2, \ldots n_2 \tag{3.69}$$

$$-\sum_{i=1}^{n_1} c_1 \frac{\partial A_1(s_i)}{\partial a_2} a_1 G_5(t_{1i}, y_{3p}) + \sum_{i=1}^{n_1} c_1 \frac{\partial B_1(s_i)}{\partial a_2} a_1 G_2(t_{1i}, y_{3p})$$
$$+\frac{1}{2}\sum_{j=1}^{n_2} c_2 \frac{\partial B_2(s_j)}{\partial a_2} a_2 G_2\left(\frac{t_{2j}}{2}, \frac{y_{3p}}{2}\right) + \frac{1}{2}\sum_{k=1}^{n_3} c_3 \frac{\partial B_3(s_k)}{\partial a_2} a_3 G_1\left(\frac{t_{3k}}{2}, \frac{y_{3p}}{2}\right)$$
$$= -\frac{1}{2}\sum_{j=1}^{n_2} c_2 B_2(s_j) L_3\left(\frac{t_{2j}}{2}, \frac{y_{3p}}{2}\right) \quad p = 1, 2, \ldots n_3. \tag{3.70}$$

The derivatives of N_{III}, N_{II1}, N_{I2} and N_{I3} with respect to a_3 can be determined in the same manner as those with respect to a_2 and the results will not be recorded here.

The analysis is therefore seen to require the solution of four simultaneous integral equations, eqns (3.23)–(3.26), to determine the stress intensity factors, given by eqns (3.31)–(3.34). In addition it is necessary to obtain the derivatives of the stress intensity factors, given by eqns (3.63)–(3.66). The number of simultaneous equations used to give three digit accuracy was about 120, where the number of equations per crack was generally taken to be proportional to the crack length. It is noted that as the ratios, h_i/b, or the ratios, h_i/h_j, $i \neq j$, become larger the accuracy tends to diminish.

4. CONCLUSIONS

When a linearly elastic brittle half-plane (solid) initially at a uniform temperature is cooled at its free surface, edge cracks may develop in the solid, which then penetrate into the half-plane as the thickness of the thermal boundary layer increases. Crack systems of this kind are governed by a strain controlled mechanism, in the sense that the total elastic energy available to induce cracking is limited, and therefore the crack extension tends to be self-arresting. It has been shown in [1] and in the present paper that the crack growth regime for this class of problems is highly affected by the interaction between adjacent cracks, as well as by the form of the temperature profile. In [1], as well as in the present paper, two temperature profiles have been considered for detailed calculation; i.e. temperature profiles given by eqns (1.1) and (1.2). However, whereas in [1] only two interacting cracks were considered, in the present work which complements [1], we have presented a detailed and complete study for three interacting cracks. On the basis of this study, the following conclusions are obtained.

1. The form of the temperature profile (the effective loading) and the interaction between adjacent cracks are the most important factors in the crack growth process.

2. If no interaction between adjacent cracks is considered (constrained stability analysis), then one may erroneously conclude in a system of parallel equally spaced edge cracks, that all cracks will grow at equal rates with increasing depth of the thermal layer. On the other hand, when interactions between two or three adjacent cracks are introduced, then qualitatively and quantitatively different results are obtained.

3. For the temperature profile (1.2) the results obtained in the present work for three interacting cracks are both qualitatively and quantitatively the same as those reported in [1] for two interacting cracks. On the other hand, for temperature profile (1.1) the results presented in this paper differ qualitatively and quantitatively from those given in [1], indicating that for this temperature profile the stability analysis based on two interacting cracks actually represents a constrained one, and therefore the true picture is obtained by the consideration of three interacting cracks, although the calculation for more than two interacting cracks requires consideration of correspondingly greater numbers of simultaneous integral equations, and therefore is considerably more complicated.

4. If only limited information is desired, then even for temperature profile (1.1) the essential features of the growth regime may be extracted by the consideration of two interacting cracks alone. As is seen from Fig. 4, the states corresponding to B, B_1, B_2, etc. can be obtained from the study of two interacting cracks (see Nemat-Nasser and Oranratnachi[10] for a more detailed discussion). Moreover, comparison between the dashed curve B_1B_2 (which is obtained for two interacting unequal cracks) and the solid curve B_1B_2 (which is obtained for three interacting unequal cracks) shows that quantitatively they are essentially the same, although qualitatively they represent completely different systems. Therefore, the spacing of the longest cracks for temperature profile (1.1) can be calculated on the basis of the information obtained for states corresponding to points B, B_1, B_2, etc. in Fig. 4. For this temperature profile, unlike that for temperature profile (1.2), no crack closure takes place: cracks grow until a critical state is reached, then alternate cracks stop growing, while the remaining ones grow at a faster rate, until a new critical state is reached, at which every other of those cracks which had continued growing stop growing, while the remaining ones continue to grow at a faster rate, and this process keeps repeating itself as the depth of the thermal layer increases.

5. Finally, we must point out that we have only considered collinear extension of equally spaced edge cracks. Crack branching and noncollinear extension have not been considered. In

this sense, therefore, our stability analysis *may* still represent a constrained one, although the essential features of the problem seem to have been revealed by our calculations.

Acknowledgements—This work was supported by National Science Foundation-RANN/ERDA Grant No. AER 75-00187 and National Science Foundation Grant No. ENG 77-22155 to Northwestern University.

REFERENCES

1. S. Nemat-Nasser, L. M. Keer and K. S. Parihar, Unstable growth of thermally induced interacting cracks in brittle solids. *Int. J. Solids Structures* **14**, 409–430 (1978).
2. S. Nemat-Nasser, *Geothermal Energy Res. Int. Memo.* (30 January 1976).
3. L. M. Keer, S. Nemat-Nasser and K. S. Parihar, Growth and Stability of Thermally Induced Interacting Cracks in Brittle Solids. *Geothermal Energy Res. Rep.*, Northwestern University (Sept. 1976).
4. S. Nemat-Nasser, Overview of the basic progress in ductile fracture (Invited Lecture), *Trans. 4th Int. Conf. Structural Mechanics in Reactor Technology* (Edited by T. A. Jaeger and B. A. Boley), Vol. L, Inelastic Analysis of Metal Structures, paper L2/1 (see Sec. 5) (1977).
5. S. Nemat-Nasser, Stability of a system of interacting cracks in combined modes. *Letters Appl. Engng Sci.* **16**, 277–285 (1978).
6. L. M. Keer and K. Chantaramungkorn, An elastic half plane weakened by a rectangular trench. *J. Appl. Mech.* **42**, 683–687 (1975).
7. G. D. Gupta and F. Erdogan, The problem of edge cracks in an infinite strip. *J. Appl. Mech.* **41**, 1001–1006 (1974).
8. F. Erdogan, G. D. Gupta and T. S. Cook, Numerical solution of singular integral equations. In *Methods of Analysis and Solutions of Crack Problems* (Edited by G. C. Sih), pp. 368–425. Noordhoff, Leyden (1972).
9. S. Krenk, On the use of the interpolation polynomial for solutions of singular integral equations. *Q. Appl. Math.* **32**, 479–485 (1975).
10. S. Nemat-Nasser and A. Oranratnachi, Minimum Spacing of Thermally Induced Cracks in Brittle Solids. Earthquake Research and Engineering Laboratory *Tech. Rep. No.* 78-1-7, Dept of Civil Engineering, Northwestern University (Jan. 1978). To be published.

APPENDIX

$$G_1\left(\frac{\pi t}{2b},\frac{\pi y}{2b}\right)=\frac{2b}{\pi}\sum_{k=-\infty}^{\infty}\left\{\frac{2(y+t)}{(y+t)^2+(2kb)^2}-\frac{(y+3t)[(y+t)^2-(2kb)^2]}{[(y+t)^2+(2kb)^2]^2}+\frac{4ty(y+t)[(y+t)^2-3(2kb)^2]}{[(y+t)^2+(2kb)^2]^3}-\frac{(y-t)[(y-t)^2+3(2kb)^2]}{[(y-t)^2+(2kb)^2]^2}\right\}$$

$$=2\coth\left[\frac{\pi}{2b}(y+t)\right]-\frac{\pi}{2b}(y+3t)\operatorname{cosech}^2\left[\frac{\pi}{2b}(y+t)\right]+4\left(\frac{\pi}{2b}\right)^2 ty\operatorname{cosech}^2\left[\frac{\pi}{2b}(y+t)\right]\coth\left[\frac{\pi}{2b}(y+t)\right]$$

$$-2\coth\left[\frac{\pi}{2b}(y-t)\right]+\frac{\pi}{2b}(y-t)\operatorname{cosech}^2\left[\frac{\pi}{2b}(y-t)\right] \tag{A1}$$

$$G_2\left(\frac{\pi t}{2b},\frac{\pi y}{2b}\right)=\frac{2b}{\pi}\sum_{k=-\infty}^{\infty}\left\{\frac{2(y+t)}{(y+t)^2+(2k-1)^2b^2}-\frac{(y+3t)[(y+t)^2-(2k-1)^2b^2]}{[(y+t)^2+(2k-1)^2b^2]^2}\right.$$

$$\left.+\frac{4ty(y+t)[(y+t)^2-3(2k-1)^2b^2]}{[(y+t)^2+(2k-1)^2b^2]^3}-\frac{(y-t)[(y-t)^2+3(2k-1)^2b^2]}{[(y-t)^2+(2k-1)^2b^2]^2}\right\}$$

$$=2\tanh\left[\frac{\pi}{2b}(y+t)\right]+\frac{\pi}{2b}(y+3t)\operatorname{sech}^2\left[\frac{\pi}{2b}(y+t)\right]-4\left(\frac{\pi}{2b}\right)^2 ty\operatorname{sech}^2\left[\frac{\pi}{2b}(y+t)\right]\tanh\left[\frac{\pi}{2b}(y+t)\right]$$

$$-2\tanh\left[\frac{\pi}{2b}(y-t)\right]-\frac{\pi}{2b}(y-t)\operatorname{sech}^2\left[\frac{\pi}{2b}(y-t)\right] \tag{A2}$$

$$G_3\left(\frac{\pi t}{2b},\frac{\pi y}{2b}\right)=\frac{2b}{\pi}\sum_{k=-\infty}^{\infty}(-1)^k\left\{\frac{(y-t)[(y+t)^2-(2kb)^2]}{[(y+t)^2+(2kb)^2]^2}+\frac{4ty(y+t)[(y+t)^2-3(2kb)^2]}{[(y+t)^2+(2kb)^2]^3}-\frac{(y-t)[(y-t)^2-(2kb)^2]}{[(y-t)^2+(2kb)^2]^2}\right\}$$

$$=\frac{\pi}{2b}(y-t)\operatorname{cosech}\left[\frac{\pi}{2b}(y+t)\right]\coth\left[\frac{\pi}{2b}(y+t)\right]+2\left(\frac{\pi}{2b}\right)^2 ty\operatorname{cosech}\left[\frac{\pi}{2b}(y+t)\right]\left\{2\coth^2\left[\frac{\pi}{2b}(y+t)\right]-1\right\}$$

$$-\frac{\pi}{2b}(y-t)\operatorname{cosech}\left[\frac{\pi}{2b}(y-t)\right]\coth\left[\frac{\pi}{2b}(y-t)\right] \tag{A3}$$

$$G_4\left(\frac{\pi t}{2b},\frac{\pi y}{2b}\right)=\frac{4b}{\pi}\sum_{k=-\infty}^{\infty}(4k+1)b\left\{-\frac{[(y+t)^2-(4k+1)^2b^2]}{[(y+t)^2+(4k+1)^2b^2]^2}+\frac{4ty[3(y+t)^2-(4k+1)^2b^2]}{[(y+t)^2+(4k+1)^2b^2]^3}+\frac{(y-t)^2-(4k+1)^2b^2}{[(y-t)^2+(4k+1)^2b^2]^2}\right\}$$

$$=\operatorname{sech}\left[\frac{\pi}{2b}(y+t)\right]-\frac{\pi}{2b}(y+t)\operatorname{sech}\left[\frac{\pi}{2b}(y+t)\right]\tanh\left[\frac{\pi}{2b}(y+t)\right]$$

$$+2\left(\frac{\pi}{2b}\right)^2 ty\operatorname{sech}\left[\frac{\pi}{2b}(y+t)\right]\left\{2\tanh^2\left[\frac{\pi}{2b}(y+t)\right]-1\right\}$$

$$-\operatorname{sech}\left[\frac{\pi}{2b}(y-t)\right]+\frac{\pi}{2b}(y-t)\operatorname{sech}\left[\frac{\pi}{2b}(y-t)\right]\tanh\left[\frac{\pi}{2b}(y-t)\right] \tag{A4}$$

$$G_5\left(\frac{\pi t}{2b}, \frac{\pi y}{2b}\right) = \frac{2b}{\pi} \sum_{k=-\infty}^{\infty} (-1)^k (2k-1) b \left\{ \frac{1}{(y+t)^2 + (2k-1)^2 b^2} - \frac{2(y-3t)(y+t)}{[(y+t)^2 + (2k-1)^2 b^2]^2} \right.$$
$$\left. - \frac{4ty[3(y+t)^2 - (2k-1)^2 b^2]}{[(y+t)^2 + (2k-1)^2 b^2]^3} + \frac{(y-t)^2 - (2k-1)^2 b^2}{[(y-t)^2 + (2k-1)^2 b^2]^2} \right\}$$
$$= -\operatorname{sech}\left[\frac{\pi}{2b}(y+t)\right] + \frac{\pi}{2b}(y-3t)\operatorname{sech}\left[\frac{\pi}{2b}(y+t)\right]\tanh\left[\frac{\pi}{2b}(y+t)\right]$$
$$+ 2\left(\frac{\pi}{2b}\right)^2 ty \operatorname{sech}\left[\frac{\pi}{2b}(y+t)\right]\left\{2\tanh^2\left[\frac{\pi}{2b}(y+t)\right] - 1\right\}$$
$$+ \operatorname{sech}\left[\frac{\pi}{2b}(y-t)\right] - \frac{\pi}{2b}(y-t)\operatorname{sech}\left[\frac{\pi}{2b}(y-t)\right]\tanh\left[\frac{\pi}{2b}(y-t)\right]. \tag{A5}$$